

High precision measurements of the $^{13}\text{CO}_2/^{12}\text{CO}_2$ isotope ratio at atmospheric pressure in human breath using a 2 μm diode laser

S.N. Andreev · E.S. Mironchuk · I.V. Nikolaev · V.N. Ochkin · M.V. Spiridonov · S.N. Tskhai

Received: 28 July 2010 / Revised version: 27 April 2011 / Published online: 10 June 2011
© Springer-Verlag 2011

Abstract A special technique is developed to measure the $^{13}\text{CO}_2/^{12}\text{CO}_2$ isotope ratio in human breath at atmospheric pressure with a 2 μm tunable diode laser. The procedure used to process the pressure-broadened spectra obtained and calculating the isotope ratio is based on a multidimensional linear regression of the spectra using simulated $^{13}\text{CO}_2$, $^{12}\text{CO}_2$, and H_2O spectra. This technique allows the measurement of the δ -value for isotopic ratios with a precision of 0.07‰ within a data acquisition time of 3 min and a long-term reproducibility of 0.2‰.

1 Introduction

The analysis of the $^{13,12}\text{C}$ concentrations is widely used in applications such as geology, volcanology, criminology, and medicine. These applications stimulate the development of novel experimental techniques capable of high precision and accuracy measurements and short data acquisition times. The best results can be obtained with isotope ratio mass analyzers used in conjunction with chromatographic gas separation. These methods can provide isotopic precision of 0.01‰ [1], but they are costly and require a large amount of space, and hence alternative methods are of great interest.

There are many practical applications that have no need for such precision. For example, the breath test precision actually required to detect the *Helicobacter Pylori* bacteria, the cause of gastric ulcers, is only 0.5‰; and the test procedure should take no more than a few minutes. Various optical

methods meeting these requirements have been discussed in the literature in recent years (see, e.g., [2]).

The most common spectroscopic techniques rely on the absorption of infrared laser radiation in vibrational-rotational transitions in CO_2 . The pertinent measurements can be performed with frequency tunable lasers using the methods of cavity ring-down spectroscopy (CRDS) [3], integrated cavity output spectroscopy (ICOS), and cavity enhanced absorption spectroscopy (CEAS) [4], wavelength modulation absorption spectroscopy (WMS) [5], and absorption with a difference frequency generation source [6].

CO_2 absorption measurements are usually taken in one of the following three spectral regions: near 4.3, 2.0, or 1.6 μm . Comparison between the CO_2 absorption features in the mid- and near-IR regions shows a significant reduction in the absorption coefficient. Specifically, the strongest lines at 1.6 μm are approximately 100 times weaker than those at 2 μm . Similarly, a 500-fold reduction is observed when changing from 4.3 to 2 μm . Therefore, the fundamental 4.3 μm band is preferred because of the high coefficient of absorption. By using a quantum-cascade laser (QCL) in highly stabilized experimental conditions (sample cell temperature and pressure), Nelson et al. [7] obtained a CO_2 isotope ratio measurement precision of 0.02‰, with a data acquisition time of 400 seconds, which is the highest precision figure achieved by spectroscopic techniques to date. However, this approach requires cryogenically cooled photodetectors, and costly of QCLs.

Lasers and detectors operating in the 1.6 μm region have advantages. They can function at room temperature and are readily available. However, due to the low CO_2 absorption coefficient in this spectral region makes it necessary to use a sample cell of 1 kilometer in optical path length. Kasyutich and coauthors [8] used a high-precision cavity for the purpose and achieved a measurement precision of 1.8‰.

S.N. Andreev · E.S. Mironchuk · I.V. Nikolaev · V.N. Ochkin · M.V. Spiridonov (✉) · S.N. Tskhai
P.N. Lebedev Physical Institute, Russian Academy of Sciences,
Leninsky Prosp. 53, Moscow 119991, Russia
e-mail: max@lebedev.ru

The 2 μm spectral region offers a practical alternative. The diode lasers and detectors operating in this region can work at room temperature, and the CO_2 absorption coefficient is sufficiently large, so that the CO_2 isotope ratio can be measured using an effective optical path length of a few meters. Such an optical path can be provided by well-engineered multipass cell. Another factor is that the water absorption lines in this region are weak.

Several publications have discussed the carbon isotope ratio measurements in the 2 μm region [9, 10]. Castrillo et al. [9] reported a long-term reproducibility of 0.5‰ for $^{13}\text{CO}_2/^{12}\text{CO}_2$ isotope ratio measurements with a DFB diode laser, with a data acquisition time of 80 minutes.

The measurement scheme used in the publication discussed above is based on a comparison between the absorption data obtained for individual molecular vibrational-rotational lines at reduced gas pressures of 10–100 Torr to minimize spectral overlapping.

Our previous work [11] differs insofar that we were able to investigate spectra consisting of congested pressure-broadened lines. We demonstrated that such an approach can also provide sufficiently high precision in spectral isotopic measurements comparable with low pressure measurements. In both cases, the precision and accuracy are limited by the comparison of the measured absorption spectral components intensities with the simulated ones; thus the same way depending on the reliability of spectral database and the possibilities of measuring technique.

The aim of present work is to demonstrate the technique of measuring the $^{13}\text{CO}_2/^{12}\text{CO}_2$ isotope ratio at atmospheric pressure to meet the needs of medical practice. Note also that the parameters most important for the above objective are the relative measurement precision and reproducibility rather than the accuracy of the absolute isotope ratio value; this being essentially individual even for a group of healthy

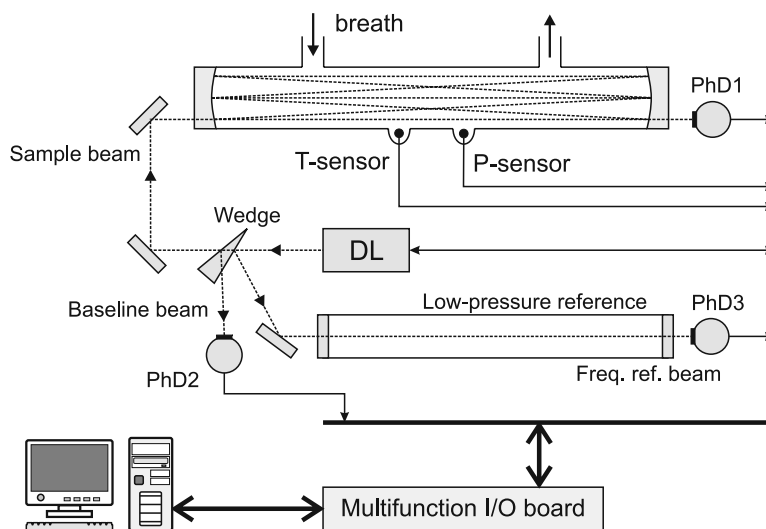
people. Bacterial diagnostics requires making reliable comparison between carbon isotope concentrations in a succession of samples of air exhaled by a selected person before and after (10 minutes to hour) taking the special isotope enriched substance. That is why we did not try to highly improve the accuracy of the absolute isotope ratio values, these being determined in some cases with the help of most simple secondary standards.

According to these objectives in Sect. 2, we describe the experimental technique and its main parameters control. Section 3 is devoted to the spectral interval choice, the necessary accuracy of frequency scale calibration, spectra processing technique, and simulations of spectral line profile. The results are presented in Sect. 4. The analysis of the precision with the help of Allan variance performed and the long term stability studied. The advantages and shortages of atmospheric pressure measurements compare to low pressure ones are discussed, and the examples of measurements are presented.

2 Experiment

The experimental setup is shown schematically in Fig. 1. The spectrometer uses a three-channel optical scheme. The probe laser beam passes through the sample channel PhD1 that includes a Herriott multipass cell containing the sample gas. The cell is 900 mm in length and with an inner diameter of 22 mm. The total optical path length in the cell is 24 m. A temperature and a pressure sensor, capable of measurement accuracies of 0.1°C and 0.2 mbar, respectively, are located inside the sample cell. The beams for the two other channels (PhD2 and PhD3) are formed by a beam-splitting wedge. The baseline channel PhD2 is needed to normalize the beam intensity in the sample channel. Channel PhD3

Fig. 1 Schematic of the experimental setup



includes a reference gas cell and is used to calibrate the laser frequency. The cell is filled with CO_2 at a pressure of 70 Torr. As shown elsewhere in the text, the accuracy of the laser frequency must be 10^{-5} cm^{-1} . This accuracy was achieved by comparing absorption spectra obtained in the reference gas cell with those tabulated for the line centers and their pressure shifts in [12]. The frequencies for the entire laser tuning curve were determined by interpolation between the reference line center positions. The interpolation procedure is discussed in Sect. 3.

The light source used in his work is a VCSEL laser diode (Vertilas) with an output power of 0.5 mW near $2.007 \mu\text{m}$. The laser is tuned by applying a periodic sawtooth injection current of up to 7 mA in amplitude and 200 Hz in repetition rate.

Control of laser frequency is an important parameter and requires stabilization of the diode laser thermoelectric cooler temperature because its typical sensitivity is $0.1 \text{ cm}^{-1}/\text{K}$. An effective stability of $3 \times 10^{-6} \text{ K}$ can be achieved [13]. In addition, we apply feedback to adjust the frequency grid to the center of absorption line of the reference gas so that a long-term (1 hour) temperature stability of 10^{-4} K is obtained for the diode laser Peltier element.

The use of the VCSEL laser offers a number of advantages. For example, its linear current-frequency tuning curve is typically wider than that of a DFB diode laser. This characteristic results in improved accuracy of the above mentioned interpolation procedure. Furthermore, the VCSEL laser beam quality facilitates obtaining similar characteristics for the split beams. The photodetectors (PhD1 through 3) used in our experimental setup are InGaAs photodiodes (Type G8372-01, Hamamatsu) followed by custom made trans-impedance amplifiers. The signals from the detectors are fed to a multifunction I/O board (Type NI-PCI-6120, 800 kHz, 16 bits, National Instruments) and computer processed using LabView 9.0 software. The absolute isotope ratio values were measured using commercially available CO_2 gas as a secondary standard. Its isotope ratio was determined with a Model MS200 quadrupole mass analyzer.

3 Details of measurement procedure.

3.1 Analytical spectral region

The diode laser, operating at a fixed temperature of 24°C was tuned in the range from 4977.4 to 4978.9 cm^{-1} based on our analysis of absorption lines intensities. In this spectral region, there are three relatively strong absorption lines of the $^{12}\text{CO}_2$ vibrational bands $\nu_1 + 2\nu_2 + \nu_3$ and $\nu_1 + 3\nu_2 + \nu_3 - \nu_2$ ($\text{R0 } 12^0_1 \leftarrow 00^0_0$, $\nu = 4978.607720 \text{ cm}^{-1}$, $\text{R17 } 13^1_1 \leftarrow 01^1_0$, $\nu = 4978.204746 \text{ cm}^{-1}$, and $\text{R16 } 13^1_1 \leftarrow 01^1_0$, $\nu = 4977.724534 \text{ cm}^{-1}$) and one line of the $^{13}\text{CO}_2$

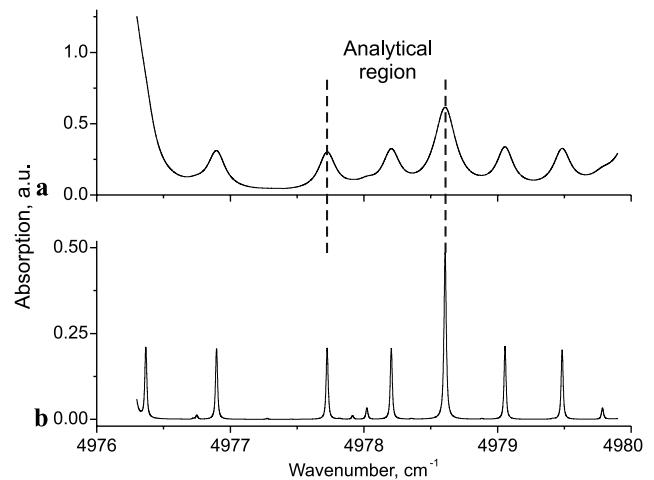


Fig. 2 Spectra recorded in (a) sample channel and (b) reference channel

vibrational band $\nu_1 + 2\nu_2 + \nu_3$ ($\text{P16 } 12^0_1 \leftarrow 00^0_0$, $\nu = 4978.022037 \text{ cm}^{-1}$). H_2O absorption lines are also observed in this spectral region at $4978.384300 \text{ cm}^{-1}$ ($000-110$ line) and $4978.499960 \text{ cm}^{-1}$ ($000-011$ line). All spectral frequencies are listed for vacuum [12]. In our previous work [11], we analyzed a much broader spectral range ($4974.5-4980.7 \text{ cm}^{-1}$), but the present experiment showed that the choice of a wider spectral region decreased the precision of the $^{13}\text{CO}_2/^{12}\text{CO}_2$ isotope ratio measurements, because the dynamic range of the absorption line intensities in this case was too large. In [11], the ratio of absorption intensities was up to 70, as compared to 15 in this work thus improves the signal/noise ratio by 2 times.

A typical example of sample and reference spectrum records is presented in Fig. 2.

3.2 Spectral processing

The procedure used to analyze spectra as recorded in the sample channel is based on multidimensional linear regression from simulated spectra of the $^{13}\text{CO}_2$, $^{12}\text{CO}_2$, and H_2O molecules:

$$\ln I_a(\nu) = \ln I_b(\nu) + \sum_i k_i \alpha_i(\nu) \cdot L + P^{(3)}(\nu), \quad (1)$$

where $I_a(\nu)$ is the signal measured in the sample channel, $I_b(\nu)$ is the signal measured in the baseline channel, $\alpha_i(\nu)$ is the simulated absorption coefficient of the i th molecule, L is the optical path length in the sample cell, k_i is the linear regression coefficient, and $P^{(3)}(\nu)$ is a cubic polynomial allowing for the residual differences between the diode laser baselines in the optical channels for PhD1 and PhD2. The result of the linear regression operation is a set of the coefficients k_i that are proportional to the concentrations of the respective molecules [11], and the ratio $k(^{13}\text{CO}_2)/k(^{12}\text{CO}_2)$

Table 1 Comparison between various interpolation techniques

Type of interpolation	δ -value precision
Linear	0.07‰
Cubic spline	0.5‰
Hermite polynomial	0.1‰

yields the desired isotope concentration ratio. The results are presented in terms of the δ -values commonly used to characterize isotope ratios:

$$^{13}\delta = \left(\frac{([^{13}\text{CO}_2]/[^{12}\text{CO}_2])_m}{([^{13}\text{CO}_2]/[^{12}\text{CO}_2])_{\text{std}}} - 1 \right) \cdot 1000\text{‰}, \quad (2)$$

where $[^{13}\text{CO}_2]/[^{12}\text{CO}_2]_m$ is the isotope ratio measured and $[^{13}\text{CO}_2]/[^{12}\text{CO}_2]_{\text{std}} = 0.011237$ is the standard (PDB) isotope ratio.

3.3 Frequency scale

Our numerical analysis and experiment show that one of the most important factors that may limit the precision in determining the $^{13}\text{CO}_2/^{12}\text{CO}_2$ concentration ratio through linear regression to simulated absorption spectra is the calibration accuracy of the diode laser frequency tuning scale. We estimate that an error of a 10^{-5} cm^{-1} in the spectral frequency leads to an error of 0.1‰ in the $^{13}\text{CO}_2/^{12}\text{CO}_2$ ratio measurement results. Hence, to achieve a δ measurement precision necessary for medical tests (0.5‰), the frequencies of the experimental absorption spectra should be locked to those of the simulated spectra with an accuracy 10^{-5} cm^{-1} . This requirement concerns the absorption line centers and is less stringent for the spectral line wings. Such an accuracy cannot be realized by means of commercially available wavelength meters. Therefore, the line center positions are determined in a low-pressure (70 Torr) reference gas cell, with corrections made for their pressure-induced shifts [12] resulting in an accuracy of 10^{-6} cm^{-1} . Subsequently, the entire diode laser frequency tuning characteristic is acquired by interpolation. Several interpolation techniques were tested; for example, linear, cubic spline, and Hermite polynomial. The best results were obtained with a linear interpolation method (see Table 1). This can probably be attributed to the limited number of reference line centers within the laser frequency tuning range. During the course of measurements, the laser frequency was repeatedly calibrated every 160 milliseconds.

3.4 Simulations of sample spectra

The spectral absorption coefficients $\alpha_i(\nu)$ for the $^{12}\text{CO}_2$, $^{13}\text{CO}_2$, and H_2O lines of interest were calculated for the comparison in the Lorentz or the Voigt approximation using

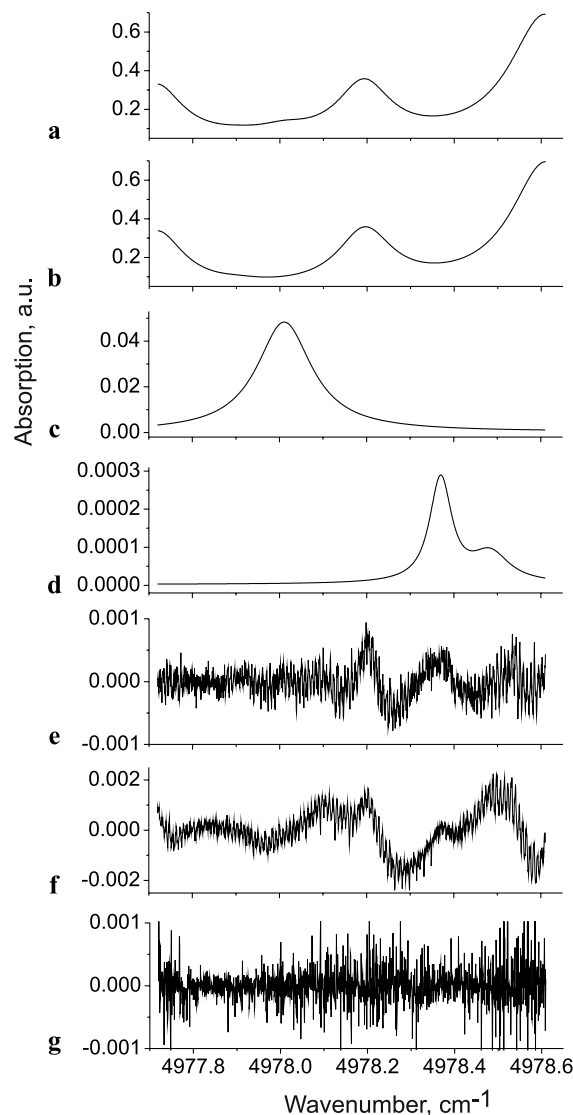


Fig. 3 CO_2 spectrum in human exhaled breath sample and the results of multidimensional linear regression. (a)—recorded spectrum; (b), (c), (d)—simulated spectra ((b)— $^{12}\text{CO}_2$, (c)— $^{13}\text{CO}_2$, (d)— H_2O); (e), (g)—regression residual for the Voigt approximation; (f)—regression residual for the Lorentz approximation. (e), (f)—signal record time 160 ms, (g)—100 s. The absorption intensity and residual scales are in arbitrary but the same units for all graphs

the HITRAN-2008 database [12]. The data from the pressure and temperature sensors installed in the multipass cell were included in the spectrum simulations. The quality of our approximation was estimated from the difference between the measured and simulated spectra, following the approximation procedure with the laser frequency tuning characteristic reconstruction method (i.e., linear interpolation).

In addition to the lines whose centers fall within the analytical spectral region (1.5 cm^{-1}), there are ten lines in the vicinity of the region ($\pm 6 \text{ cm}^{-1}$) that were also included in our simulations in order to allow for contributions from the spectral wings to the analytical line profile.

Figure 3 presents an example of application of the regression procedure to a CO_2 spectrum from human breath. Presented are the results for both the Lorentz and the Voigt approximation of the simulated spectra. One can see that the Voigt approximation (curves e, d) yields a much smaller residual difference between the spectrum recorded and the sum $\sum k_i \alpha_i(\nu)L$ for the $^{12}\text{CO}_2$, $^{13}\text{CO}_2$, and H_2O molecules than that in the case of the Lorentz approximation (curve f). In case of the Voigt approximation, the residual difference for the total absorption coefficient is $<10^{-3}$ of the measured spectrum intensity. There are two graphs of the residual for Voigt profile. Graph (e) refers to averaging for 160 ms (a single laser frequency tuning cycle, 64 pulses) and graph (g) refers to 100 s averaging. It is apparent that curves (e) and (g) are not spectrally correlated. This implies that the regular residual between the calculated Voigt profile and the measured spectrum not observed at the level of the measurements precision. At the same time, a residual fine structure with a spacing of 0.008 cm^{-1} is apparent. We attribute this fine structure to interference fringes introduced by the optical system.

Further improvements were made to our spectral simulation. All known broadening mechanisms in linear optics (except for molecular processes which may be significant when the line broadening is comparable with transition frequency) were considered specifically Dicke narrowing. Since this narrowing affects only the Gaussian component of the Voigt profile, we varied (not according to the temperature sensor data) the width of the Gaussian profile component down to 50% of its real Doppler value. However, the residual difference between the measured and simulated spectra decreased most likely due to the finite accuracies of the HITRAN spectral database [12] and our frequency scale calibration.

The above mentioned residual difference value of 10^{-3} cm^{-1} corresponds to the precision of the δ -value measurements. To determine the real precision, it is necessary to apply statistical processing, which will be considered in the next section.

4 Results and discussion

4.1 Measurements precision

The δ -value precision was estimated using the Allan variance [14]. Figure 4 depicts the Allan deviation plot and demonstrates a 0.07‰ δ -value precision obtained from human breath measurements with an averaging time of 3 minutes. This precision was defined for a time at which the Allan plot fluctuations are a factor 2 above the minimum of the curve shown in Fig. 4. This precision level is comparable to that obtained using an isotope mass analyzer.

Our precision level is higher than that reported in the majority of previous work reported [2] which were measured

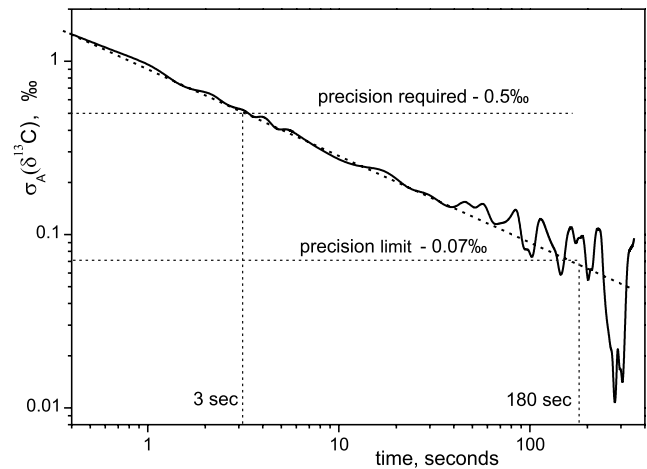


Fig. 4 Allan deviation plot for the $\delta^{13}\text{C}$ isotope ratio

at low sample gas pressures in order to achieve spectral resolution. Hence, the δ -values were obtained from a limited number of narrow line centers. Furthermore, two gas cells were used to measure the difference in δ , one of the cells being used as a secondary isotope standard.

In addition to its capability of being used at atmospheric pressure, i.e., with no need for vacuum equipment, our approach suggested offers the following advantages:

- The regression scheme involves a large array of spectral fragments, including not only the central parts of the lines of interest, but also overlapped parts of the spectrum and line wings, which improves the statistics.
- There is no need for the gas temperature and pressure in the sample and the reference cells to be identical, as the latter is only used for laser frequency calibration. It is well known that fluctuations of the Boltzmann factor due to temperature variations have a strong influence on the δ -value measurement results. Castrillo and coworkers [9] and Gagliardi et al. [10] reported an 11‰ K^{-1} measurement accuracy obtained in the $2\text{ }\mu\text{m}$ spectral region (8‰ K^{-1} accuracy in this work due to the optimization of the analytical spectral region). The temperature and gas density variations are recorded by the sensors and are taken into account in our spectral simulations. In our approach, it is necessary to measure the temperature in the sample cell, rather than stabilize it. Figure 5 presents an example of a sample gas temperature record plotted with a time resolution of $5 \times 10^{-3}\text{ s}$. The temperature fluctuations are below the minimum of the absolute accuracy of the sensors (see Sect. 2) allows them to record. Typical slow temperature fluctuations are on the order of 0.03 K and occur on a time scale of 10 to 100 s (which can be taken into account since the characteristic regression cycle time is around 0.2 s). Noise-like fluctuations are on the order of 0.001 K , and their influence should not exceed 0.01‰ . The possible

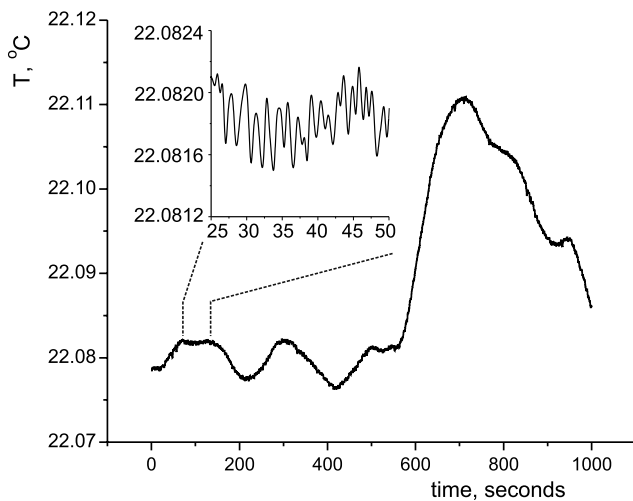


Fig. 5 Temperature fluctuations in the sample cell

effect of slow temperature fluctuations on the isotope ratio measurement precision is no more than 0.3‰ in our experimental conditions. The typical parameters plotted in Fig. 5 for a 6-min interval remain the same for much longer times, say, on the order of tens of hours.

- (c) Data obtained from smoothed spectra should be less sensitive to the effect of experimental uncertainties.
- (d) The Dicke narrowing (DN) effect appears when the absorbing molecule mean free path became comparable to the absorption wavelength. For $\text{CO}_2\text{-N}_2$ collisions and a 2 μm wavelength such condition correspond to a pressure of 30 Torr. DN influences the Doppler component and converts it from Gaussian to dispersive profile [15], and thus disturbs the Voigt profile. The influence is more pronounced when the input of the Doppler component to the Voigt convolution is relevant. For the lines under consideration, the Doppler to Lorentz widths ratio $\Delta\nu_D/\Delta\nu_L$ at 300 K is 0.15 to 0.07 at atmospheric pressure and 2.5 to 1 at 50 Torr. In this case, our situation results at elevated pressure is less sensitive to line profile models such as Galatry or Rautian–Sobelman models as compare to the Voigt profile model (see the results in Sect. 3.4). For these more sophisticated models, new fitting parameters for DN are needed [16, 17]. For collision broadening and shift data adapted to standard atmospheric pressure and composition can be taken from HITRAN [12] to include the dependence on the rotational state for the standard air (nitrogen, oxygen, argon, water, etc.) for both ($^{12,13}\text{C}$) carbon dioxide isotopomers. The HITRAN database contains the information for CO_2 self broadening parameters which allows correction of the broadening factors for exhaled breath compared to standard air. Even small changes in the oxygen density in the breath can be compensated by nitrogen at fixed pressure and the broadening factors for

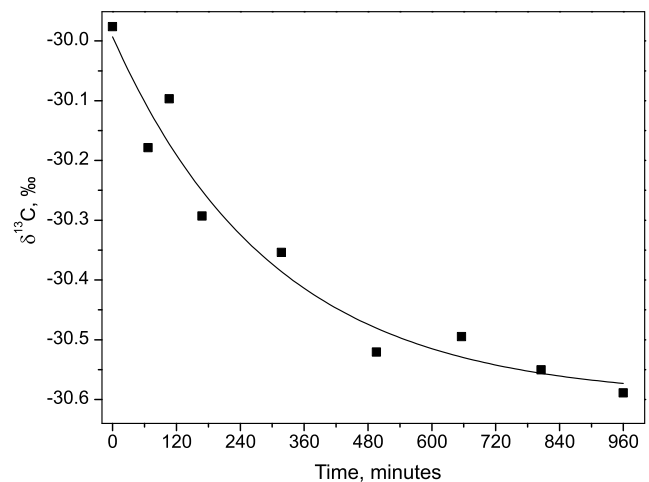


Fig. 6 Long-term (16-hr) reproducibility for $\delta^{13}\text{CO}_2$

these molecules are almost equal. The influence of water line wings was also accounted (see Sect. 3.4). Precise spectrum simulations require accuracy of the experimental frequency scale. This limits precision and accuracy, and hence the progress in precision demonstrated in this work seems is the result of a trade-off of this factor and factors (a) to (d) above.

4.2 Accuracy and reproducibility

As far as exhaled breath tests are concerned, the long-term reproducibility of carbon isotope ratio measurements is an important parameter, because the test procedure involves comparison between two exhaled air samples taken and measured at different times. To estimate the accuracy and long-term stability of the analyzer breath samples acquired for 16 hours. The results of these δ -value measurements are presented in Fig. 6. It can be seen that during this time interval the total variance of the δ -values reached 0.6‰, with a standard deviation of 0.2‰. Figure 6 shows that the analyzer does not deviate from a CO_2 isotopic ratio of $<0.015\%$ in a data acquisition time of 1 hr.

The δ -values shown in Fig. 6 represent absolute deviations from the PDB standard [2]. To obtain these data, we calibrated our diode laser based analyzer using commercially available CO_2 gas as a secondary standard. The isotope ratio in this gas was determined with a Model MS200 quadrupole mass analyzer. The δ -value deviation was measured at $+(18 \pm 3)\%$ relative to the PDB value. A corresponding correction was applied to our absolute optical measurements.

A comparison of the techniques used and results in this work with those for our earlier work (precision 0.4‰) [11], as well as for pressure-broadened lines, shows that the precision improvement primarily due to the optimization of the analytical spectral interval and the use of temperature and

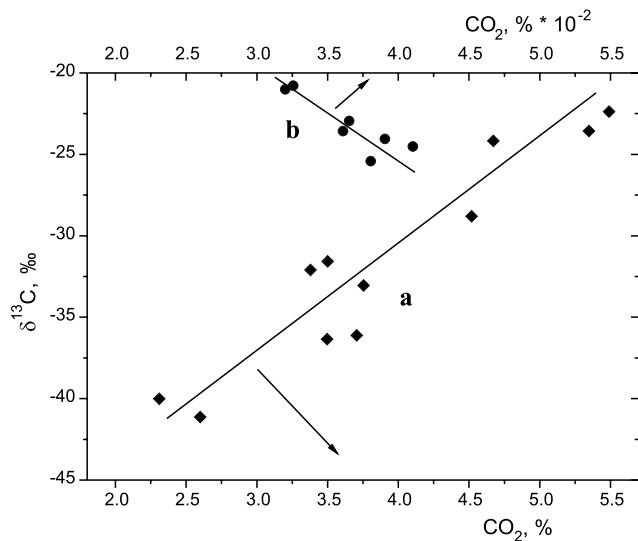


Fig. 7 Example of exhaled breath measurements. (a) $\delta^{13}\text{CO}_2$ as a function of the total CO_2 concentration in the exhaled breath sample from 5 persons; (b) the same for plants [18]

pressure sensors in the sample cell. Further improvement can be achieved by means of optimization of a multipass Herriott cell geometry designed for suppressing the influence of residual interference fringes. Figure 7a illustrates an example of isotope δ -value measurements in exhaled breath samples taken from a group of 5 people. The measurements were taken at different instants of time during the course of a day. In that case, no measures were taken to control the depth of inhalation, breath holding, and the other sampling details. Also measured at the same instant of time was the total carbon dioxide concentration (μ , %) in the exhaled breath samples. Although the δ - and μ -values for each subject are individual, their correlation can be seen in Fig. 7. The deviation of the isotope ratio δ from the standard value decreases with increasing carbon dioxide concentration in the exhaled breath. The objective of these experiments was to show the existence of correlation between the absolute carbon dioxide concentration and isotope ratio. The existence of correlation between these values was reported in [18] concerned with geochemical analyses of air near plants. The relationship between δ and μ for plants is illustrated by the graph in Fig. 7b. In this case, the correlation is the opposite for that for humans, considering that plants consume carbon dioxide, whereas humans produce it.

5 Conclusions

The results presented in this work focuses on the precision of optical measurements of carbon isotope ratio in exhaled breath at atmospheric pressure. A diode laser operating in the $2\ \mu\text{m}$ spectral region is used to perform stable and precise

measurements of relative changes in the carbon isotope ratio δ as required by medical bacterial diagnostics. The δ -value precision determined by means of the Allan deviation plot with an averaging time of 3 minutes was 0.07‰ . Such precision is comparable with that provided by modern isotope mass analyzers. The standard deviation of the δ -value measured for 16 hours was no more than 0.2‰ , without thermal and mechanical isolation and stabilization of the experimental setup. A correlation was observed between the δ -value and the total CO_2 concentration in the exhaled breath.

Acknowledgements This work was partially supported by the Russian Foundation for Basic Research (RFBR Grants 11-08-01127-a, 10-02-01111-a, and 10-08-00687-a).

References

1. P. Ghosh, W.A. Brand, *Int. J. Mass Spectrom.* **228**, 1 (2003)
2. E. Kerstel, L. Gianfrani, *Appl. Phys. B* **92**, 439 (2008)
3. E.H. Wahl, B. Fidric, C.W. Rella, S. Koulikov, B. Kharlamov, S. Tan, A.A. Kachanov, B.A. Richman, E.R. Crosson, B.A. Paldus, S. Kalaskar, D.R. Bowling, *Isot. Environ. Health Stud.* **42**, 21 (2006)
4. R. Wehr, S. Kassi, D. Romanini, L. Gianfrani, *Appl. Phys. B* **92**, 459 (2008)
5. G.B. Rieker, J.B. Jeffries, R.K. Hanson, *Appl. Phys. B* **94**, 51 (2009)
6. D. Richter, B.P. Wert, A. Fried, P. Weibring, J.G. Walega, J.W.C. White, B.H. Vaughn, F.K. Tittel, *Opt. Lett.* **34**, 172 (2009)
7. D.D. Nelson, J.B. McManus, S.C. Herndon, M.S. Zahniser, B. Tuzson, L. Emmenegger, *Appl. Phys. B* **90**, 301 (2008)
8. V.L. Kasyutich, P.A. Martin, R.J. Holdsworth, *Appl. Phys. B* **85**, 413 (2006)
9. A. Castrillo, G. Casa, E. Kerstel, L. Gianfrani, *Appl. Phys. B* **81**, 863 (2005)
10. G. Gagliardi, R. Restrieri, G. Gasa, L. Gianfrani, *Opt. Lasers Eng.* **37**, 131 (2002)
11. E.S. Mironchuk, I.V. Nikolaev, V.N. Ochkin, S.S. Rodionova, M.V. Spiridonov, S.N. Tskhai, *Quantum Electron.* **39**, 388 (2009)
12. L.S. Rothman, I.E. Gordon, A. Barbe, D.C. Benner, P.F. Bernath, M. Birk, V. Boudon, L.R. Brown, A. Campargue, J.-P. Champion, K. Chance, L.H. Coudert, V. Dana, V.M. Devi, S. Fally, J.-M. Flaud, R.R. Gamache, A. Goldman, D. Jacquemart, I. Kleiner, N. Lacome, W.J. Lafferty, J.-Y. Mandin, S.T. Massie, S.N. Mikhailenko, C.E. Miller, N. Moazzen-Ahmadi, O.V. Naumenko, A.V. Nikitin, J. Orphal, V.I. Perevalov, A. Perrin, A. Predoi-Cross, C.P. Rinsland, M. Rotger, M. Simeckova, M.A.H. Smith, K. Sung, S.A. Tashkun, J. Tennyson, R.A. Toth, A.C. Vandaele, J. Vander Auwera, J. Quant. Spectrosc. Radiat. Transf. **110**, 533 (2009)
13. T.M. Shay, Y.C. Chung, *Opt. Eng.* **29**, 681 (1990)
14. P. Werle, R. Muecke, F. Slemr, *Appl. Phys. B* **57**, 131 (1993)
15. V.N. Ochkin, *Spectroscopy of Low Temperature Plasma* (Wiley-VCH, New York, 2009), p. 609
16. J.W. Brault, L.R. Brown, C. Chackerian, R. Freedman, A. Predoi-Cross, A.S. Pine, *J. Mol. Spectrosc.* **222**, 220 (2003)
17. E.R. Crosson, K.N. Ricci, B.A. Richman, F.C. Chilese, T.G. Owano, R.A. Provencal, M.W. Todd, J. Glasser, A.A. Kachanov, B.A. Paldus, T.G. Spence, R.N. Zare, *Anal. Chem.* **74**, 2003 (2002)
18. E.M. Galimov, *Geochemistry of Stable Carbon Isotopes* (Nauka, Moscow, 1968) (in Russian)